Computational Investigation of Isoeugenol Transformations
on a Platinum Cluster – II: Deoxygenation through
Hydrogenation to Propylcyclohexane

Chiara Nania[a], Francesco Ferrante[a,*], Marco Bertini[a], Laura Gueci[a], Dario Duca[a]

[a]*Dipartimento di Fisica e Chimica "E. Segrè" - Università degli Studi di Palermo, Viale delle Scienze Ed. 17, I-90128 Palermo, Italy*

Abstract

The debate on climate change and the future of our Planet has brought to general attention the problem of fossil fuels (coal, oil and natural gas), among the main causes of Earth's pollution. At the same time, the necessity to encourage research and development of alternative and renewable energy resources has become increasingly relevant. In this context, biomass is an attractive option to produce biofuels and chemicals currently derived from petroleum. The hydrodeoxygenation process of bio-oils, produced by the rapid pyrolysis of biomass, is the most effective strategy for obtaining biofuels, hence the reason for the investigation of its mechanism on model biomass compounds. Having investigated the direct deoxygenation (DDO) mechanims in the first paper of this series, the present work aims to illustrate the deoxygenation-through-hydrogenation (HYD) mechanism, by which isoeugenol, a compound chosen as a model of bio-oils, is converted into propylcyclohexane on a ten-atom platinum cluster. DFT calculations highlight, from kinetic and thermodynamic perspectives, how the formation of propylcyclohexane takes place through 4-propyl-2-methoxycyclohexane-1-ol the removal of $-OCH_3$ as methanol and then of the

---

[*]Corresponding author

Email addresses: `chiara.nania@unipa.it` (Chiara Nania), `francesco.ferrante@unipa.it` (Francesco Ferrante), `marco.bertini@unipa.it` (Marco Bertini), `laura.gueci@unipa.it` (Laura Gueci), `dario.duca@unipa.it` (Dario Duca)

−OH group as water. Microkinetic analysis, performed by joining findings on both DDO and HYD routes, reveals that the isoeugenol DDO mechanism is favored at any selected temperatures.

1. Introduction

The impending depletion of fossil fuels, joined to the growing concerns for environmental protection, increases the global demand for renewable energy [1, 2]. Lignocellulosic biomass has been identified as an attractive feedstock for the production of biofuels and chemicals because the involved energy can be harnessed directly by combustion or indirectly by conversion to gas or liquid fuel [3, 4]. Among the several biomass conversion technologies, rapid pyrolysis followed by hydrodeoxygenation (HDO) of the produced bio-oil has received the most attention because it is capable of transforming the solid and low-density biomass into a vehicle fuel that is CO_2-neutral and not affected by SO_x emissions, in virtue of its negligible sulfur content [5, 6]. Through pyrolysis, essentially any biomass source can be converted into bio-oil. Although remarkably more energy dense than the original biomass, bio-oil has a low calorific value compared to crude oil, a low shelf life, and it is viscous and polar, making it unsuitable as motor fuel [7, 8]. These characteristics are all associated with the high water and oxygen content in bio-oil. However, because bio-oil has a higher volumetric energy density and is easier to handle than biomass, it is more suitable for transportation and further processing [9, 10]. The purpose of upgrading these oils is therefore to remove oxygenated groups so as to increase thermal and chemical stability, heating value and volatility [11–13]. Among the suitable methods to achieve these goals, the HDO process, which involves the challenging C-O bond cleavage reaction, is considered the most efficient technology [14–16]. Since the mixtures of several hundred compounds can be extracted from biomass, the only possible strategy to better understand the catalytic upgrading process involves mechanistic investigation of model compounds representative of lignocellulosic

biomass, such as phenolic compounds (isoeugenol, guaiacol, anisole, phenol) [5, 17].

Several reaction pathways have been proposed in the literature for the HDO of phenolic derivatives: (i) hydrogenation followed by deoxygenation (HYD), which is based on sequential hydrogenation of the aromatic ring followed by removal of the oxygenated groups; (ii) direct deoxygenation (DDO) in which there is first dissociation of the C-O bonds and then hydrogenation of the benzene ring; and (iii) tautomerization [18, 19]. In our previous study, hencefort indicated as paper I [20], a computational mechanistic analysis of the HDO reaction of isoeugenol on platinum cluster Pt_{10} was carried out following the DDO mechanism mentioned above. In the present study the investigation of the branching reaction pathways that ponder the HYD-type mechanisms is reported, as part of a broader project which has the purpose to completely elucidate the entire reaction path, characterizing the HDO process on a subnanometer platinum catalyst in the presence of molecular hydrogen. The knowledge of the HDO atomistically-detailed mechanism as occurring on the isolated cluster allows one to discriminate the most important elementary steps, thus creating a reference for computational investigations on clusters in the subnanometric size regime. This could pave the way to corresponding, more cumbersome, studies on supported clusters [21–24] under molecular hydrogen. In fact, the experimental countepart of the catalytic model employed in the present study could be the atomically precise subnanometer platinum clusters (Pt_n, with n = 5–13) supported on carbon black, obtained by Imaoka *et al.* [25] by low-temperature calcination of platinum organothiolate complexes under hydrogen stream.

2. Computational Details and Models

All the calculations were performed using density functional theory (DFT) as implemented in the Gaussian 16 package [26]. The B3LYP hybrid exchange-correlation functional [27] was used joined with the D3 correction scheme developed by Grimme (GD3) [28], which allows to empirically correct for the

contribution of dispersion interactions. The study of HDO reaction on the platinum cluster was carried out by using the LANL2DZ basis set [29, 30]; this employs Dunning's basis set (D95) [31] for light atoms and a double-zeta valence basis set associated to an effective core potential for platinum. Primitive gaussians with the role of polarization functions were added to light atoms in accordance with the following scheme: H (s: 0.049, p: 0.587), C (p: 0.0311, d: 0.587), O (p: 0.0673, d: 0.961). The values of the exponents were taken from the EMSL Basis Set Exchange website [32]. Minima and transition state (TS) species on the reaction pathways were checked by inspection of the harmonic vibrational frequencies. The energetics of the investigated reaction pathways are accordingly reported in terms of vibrational zero-point corrected energies (E_{ZPV}). Desorption energies were corrected for the basis set superposition error (BSSE) by using the counterpoise method of Boys and Bernardi[33]; given that BSSE values were calculated as correction to the SCF eneriesy, they are reported in parentheses together with the uncorrected E_{ZPV} energies.

A regular tetracapped octahedron platinum cluster shaped by ten atoms (considered as a magic number [34]), having T_d symmetry and spin multiplicity equal to 9 was chosen as subnanometric catalyst model. According to DFT calculations reported in the literature [35], this Pt_{10} cluster is a global minimum in its potential energy surface. Its structure shows the presence of atoms with different coordination: the four cap atoms actually have coordination number (CN) 3, and the remaining six atoms have CN 6 [17, 20]. In passing, it is recalled that, in the work of Imaoka *et al.* [25], Pt_{10} resulted to be the most active catalyst for stirene hydrogenation, supporting the here modeling choice.

Finally, it has to be noted that two assumptions, commonly performed in investigations like the present one, persist: i) the H_2 molecule easily breaks on the cluster with minimal activation energy, allowing atomic hydrogen to diffuse freely and be available where needed; the validity of this assumption for Pt_{10} was, in particular, confirmed in paper I, and ii) the barriers for overcoming possible geometric rearrangments of intermediates and fragments on the cluster are lower than the energy barriers related with their transformations.

4

3. Results and Discussion

The HYD mechanism of isoeugenol involves, after the formation of dihydroeugenol by hydrogenation of the double bond on the allyl chain, the complete hydrogenation of the aromatic ring and next the removal of the oxygenated groups. As illustrated in Scheme 1, the sequence of the chemical intermediates from 4-propyl-2-methoxycyclohexan-1-ol indicates four distinct routes for removing the oxygenated groups to obtain propylcyclohexane. These routes are briefly summarized below

- **HYD-1** involves the removal of the OCH_3 group as methanol and the subsequent water loss, from 4-propylcyclohexan-1-ol.

- **HYD-2** involves initially the elimination of $-OH$ as water, resulting in 1-methoxy-3-propylcyclohexane, from which methanol is removed to form propylcyclohexane.

- **HYD-3** involves the formation of 3-propylcyclohexan-1-ol by conversion of the OCH_3 fragment to OH due to the elimination of the $-CH_3$ fragment as methane and the hydrogenation of the dangling oxygen in the adsorbed structure.

- **HYD-4** involves the formation of 4-propylcyclohexane-1,2-diol, which leads to propylcyclohexane by subsequent elimination of two water molecules.

[Scheme 1 about here.]

The ring saturation follows a Horiuti-Polanyi scheme, involving the consecutive addition of hydrogen adatoms [36]. It was observed that, after the first H atom is added, the subsequent addition of atoms always occurs at the *ortho* position to the pre-existing one(s), see Figure 1. For the addition of the first H atom, all carbon sites in the ring were considered as potentially hydrogenable. The calculated values for the energy barriers and relative stabilities of the intermediates suggest that the first site to undergo hydrogenation is C3; an energy barrier of 105.0 kJ mol^{-1} is required for this process. In agreement with the

observation above, the two ortho positions at C3 were taken into account for the addition of the second H atom. Following Figure 1, hydrogenation on C2 appears significantly favored because of a lower energy barrier (57.0 vs. 127 kJ mol^{-1}) and a higher stability of the resulting intermediate **II**, the 6-methoxy-4-propylcyclohexa-1,3-dien-1-ol/Pt$_{10}$, species (43.6 vs. 57.0 kJ mol^{-1}). For the latter, a desorption energy from the cluster of 262.5 (BSSE = 31.1) kJ mol^{-1} was calculated. For the addition of the next H atom, the carbon atoms C1 and C4 were considered as reactive centers to originate intermediate III. Hydrogenation on C1 however appeared quite favored by virtue of a larger stability, about 48.0 kJ mol^{-1}. An activation barrier of 71.9 kJ mol^{-1} governs the formation of intermediate **IV** (6-methoxy-4-propylcyclohex-3-en-1-ol/Pt$_{10}$), from which by hydrogenation of C4, and crossing an energy barrier of 45.7 kJ mol^{-1}, intermediate **V** is obtained. Finally, the last H atom added on C5 leads to the formation of 2-methoxy-4-propylcyclohexan-1-ol/Pt$_{10}$ surface species, which is at an energy of 69.9 kJ mol^{-1} with respect to the species **IV+2H**. It is worth to note that an activation barrier of 39.3 kJ mol^{-1} is required for this last step, which is significantly lower than those calculated for the hydrogenations of the individual carbon atoms of the ring.

In agreement to what is known about substituents effects in aromatic reactions, the ring carbon atoms that preferentially undergo hydrogenation are those at the *ortho* and *para* positions to the oxygenated substituents. By pushing electronic density, these latters make in fact the ring more reactive to the attack of a hydrogen atom. We can conclude, however, that hydrogenation of dihydroeugenol is disadvantaged if compared to propylbenzene hydrogenation, which has been pursued in DDO mechanisms (paper I). This may be due to greater substrate-cluster interactions when oxygenated groups are present, resulting, among the other effects, also from the high fluxionality of the platinum cluster. Furthermore, another effect contributing to the inhibition of the hydrogenation can be also invoked: in isoeugenol, the *ortho* position with respect to one oxygenated site corresponds to the *meta* position with respect to the other oxygenated one, so partially eliminating the beneficial effect on the fragment

reactivity arose from the electron density donation.

[Figure 1 about here.]

3.1. HYD-1

This mechanism (represented in Figure 2) first implies the removal of methanol determining the production of 4-propylcyclohexan-1-ol followed by the formation of propylcyclohexane caused by the expulsion of one H_2O molecule. The first elementary step involves, by crossing an energy barrier of 149.2 kJ mol^{-1}, the cleavage of the C2$-$O bond in the 2-methoxy-4-propylcyclohexan-1-ol with chemisorption of the OCH$_3$ fragment between the two metal centers of the upper portion of a cluster edge. By comparison, in the loss of OCH$_3$ from dihydroeugenol (paper I), the energy of the transition state is sensibly higher (by ca. 40 kJ mol^{-1}) but the reaction is significantly more exothermic (again, by ca. 40 kJ mol^{-1}). This could be because, in the case of 2-methoxy-4-propylcyclohexan-1-ol, in the TS there is no stabilization due to the hydrogen bonds interactions, as the OH group is engaged with the metal, while the product is much more stable than the reactant because the O$-$Pt interaction is replaced by the stronger C$-$Pt one. The (int1+CH$_3$O)/Pt$_{10}$ intermediate, formed following an energy release of 60.5 kJ mol^{-1}, undergoes the fragmentation of a H_2 molecule, required to proceed with the reaction. Thus, in the second elementary step, hydrogenation of the CH$_3$O fragment occurs with formation of the CH$_3$OH molecule, for which a desorption energy of 89.7 (BSSE = 8.9) kJ mol^{-1} was calculated. The int1/Pt$_{10}$H species, through the hydrogenation on unsaturated C2, leads to the formation of the 4-propylcyclohexan-1-ol, for which the calculated desorption energy is 138.3 kJ mol^{-1} (BSSE = 20.6 kJ mol^{-1}). The latter is lower than the energy barrier of the next stage (178.0 kJ mol^{-1}) that, by C1$-$OH bond breakage, leads to propylcyclohexane. This would seem to suggest that just a small fraction of molecules should be able to acquire the sufficient energy for proceeding with the reaction. The 178 kJ mol^{-1} barrier is in fact much higher than the one relating to the dehydroxylation of propylphenol (115 kJ mol^{-1},

7

paper I). This may be due to the fact that, while in the case of propylphenol the molecule was strongly interacting with the cluster by virtue of the presence of the phenyl, in this case, due to the steric hindrance along with the weak interactions between the cyclohexane residue and the cluster — mainly caused by the lack of the anchoring effect owing to the absence of the fragment containing the hydroxyl oxygen — the migration of the OH group occurs between two terminal fragments well-nigh separated from each other. The resulting $(int2+OH)/Pt_{10}$ species is characterized by the presence of the OH fragment placed between two Pt atoms on an edge of the cluster, and by int2 interacting only via C1 with the platinum atom at the apical position.

[Figure 2 about here.]

The fragmentation of an additional H_2 molecule enables the desorption of water and the formation of propylcyclohexane. Therefore, an H atom is added to the oxygen atom of the OH fragment (energy barrier of 87.7 kJ mol^{-1}) with an energy release of 12.2 kJ mol^{-1} for the formation of the $(int2+H_2O)/Pt_{10}$ species. From the latter there is desorption of the H_2O molecule, a process whereby the calculated energy is 37.8 kJ mol^{-1} with a BSSE of 5.4 kJ mol^{-1}. The other adatom, by crossing an energy barrier of 47.9 kJ mol^{-1}, is responsible for the formation of propylcyclohexane/Pt_{10}; the calculated energy for its desorption was 97.5 (BSSE = 21.1) kJ mol^{-1}.

3.2. HYD-2 and HYD-3

The second reaction pathway involves the elimination of the $-OH$ group as water with the formation of 1-methoxy-3-propylcyclohexane, from which elimination of methanol follows, leading to propylcyclohexane. The first elementary surface transformation, characterized by an energy barrier of 164.0 kJ mol^{-1}, concerns the cleavage of the $C1-O$ bond in the 2-methoxy-4-propylcyclohexane-1-ol and leads, with a considerable energy release of 95.2 kJ mol^{-1}, to the $(int3+OH)/Pt_{10}$ species (Figure 3). On th platinum cluster, in order to proceed with the reaction, a H_2 molecule is fragmented. In the next elemen-

8

tary step, there is an H-atom migration from the cluster to the unsaturated C1 (energy barrier of 100.8 kJ mol^{-1}) with formation of the 1-methoxy-3-propylcyclohexane/Pt$_{10}$, with the molecular species that can desorb from the cluster clearing an energy barrier of 139.6 (BSSE = 21.9) kJ mol^{-1}.

[Figure 3 about here.]

From the 1-methoxy-3-propylcyclohexane/Pt$_{10}$ the removal of the $-$OCH$_3$ fragment might lead to the production of methanol or methane wherein the oxygen atom remains dangling. In the former case there is cleavage of the C$-$OCH$_3$ bond, characterized by an energy barrier of 192.6 kJ mol^{-1}, with formation of the (int4+OCH$_3$)/Pt$_{10}$ species. From this, in turn, by hydrogenation of the OCH$_3$ fragment and subsequent transfer of one H atom to the unsaturated carbon atom, propylcyclohexane/Pt$_{10}$ is obtained (Figure 3).

The second case defines the HYD-3 mechanism, reported in Figure 4, where the cleavage of the O$-$CH$_3$ bond requires the overcoming of an energy barrier of 180.5 kJ mol^{-1}, leading to the formation of the (int5+CH$_3$)/Pt$_{10}$ species. This is less stable than the previous intermediate by about 52 kJ mol^{-1}. From the species (int5+CH$_3$)/Pt$_{10}$ thus the elimination of methane by hydrogenation of the CH$_3$ fragment occurs, followed by the hydrogenation of the dangling oxygen belonging to the int5 species. The next step, which is characterized by an energy barrier of 118.4 kJ mol^{-1}, leads to the formation of 3-propylcyclohexane-1-ol/Pt$_{10}$ from which, chemisorbed propylcyclohexane is generated *via* loss of a H$_2$O molecule and saturation of C1.

[Figure 4 about here.]

3.3. HYD-4

The HYD-4 mechanism considers the removal of methane from 2-methoxy-4-propylcyclohexane-1-ol and the formation of 4-propylcyclohexane-1,2-diol whence, by elimination of two H$_2$O molecules, propylcyclohexane is obtained. The first elementary step involves, through crossing an energy barrier of 164.6 kJ mol^{-1},

9

the cleavage of the $O-CH_3$ bond with formation of the $(int7+CH_3)/Pt_{10}$ species (Figure 4). The latter is characterized by the CH_3 fragment adsorbed on the Pt atom at the apical position and the int7 species interacting through the two oxygen atoms with Pt centers showing different coordinations. Methane generation occurs, after fragmentation of a H_2 molecule on the cluster, by transfer of a single H atom to the carbon of the CH_3 fragment. As a result of CH_4 desorption, the $int7/Pt_{10}H$ species marked by the presence of a dangling O atom is obtained. From $int7/Pt_{10}H$ there is the hydrogenation of oxygen atom to form the 4-propylcyclohexane-1,2-diol/Pt_{10} species, for which the calculated desorption energy is 126.2 kJ mol^{-1} with BSSE = 24.3 kJ mol^{-1} (see Figure 5).

[Figure 5 about here.]

Breakage of the $C-OH$ bond in para position with respect to the propyl chain after occurs on the 4-propylcyclohexane-1,2-diol/Pt_{10} species, an event for which an energy barrier of 161.0 kJ mol^{-1} must be overcome. The resulting species, $(int1+OH)/Pt_{10}$ — being int1 the same residue appearing in the HYD-1 mechanism, Figure 2, but coadsorbed with OH — is more stable than 4-propylcyclohexane-1,2-diol/Pt_{10} by ca. 99 kJ mol^{-1}. A new H_2 molecule is then fragmented on the cluster in order to remove water thus obtaining propylcyclohexanol.

Hence, after that another hydrogen molecule fragments on the cluster, there is the H atom transfer to the O atom of the OH fragment (energy barrier equal to 106.3 kJ mol^{-1}) with the subsequent H_2O formation. Following its desorption from the cluster, the remaining $int1/Pt_{10}H$ species connects HYD-4 to the already discussed HYD-1 mechanism.

4. Kinetic Analysis

In the previous section we discussed the four possible routes, according to the HYD mechanism, for the conversion of isoeugenol to propylcyclohexane on the Pt_{10} cluster. In the first part of the series (paper I), some of the possible

routes within the DDO mechanism were detailed [20]. One of these pathways, specifically the DDO-2 route, was further analyzed to ensure comparability and, consequently, discrimination between the two mechanisms, namely DDO and HYD, in terms of both kinetic and thermodynamic aspects. The energetics of the eigth pathways of the two alternative mechanisms, schematized in Figure 6, suggest, based exclusively on the relative energetics of minima and transition states, that in the early elementary phases following dihydroeugenol formation, hydrogenation of the phenyl ring would appear to be kinetically favored with respect to deoxygenation. Conversely, the latter would seem to be more probable to occur from dihydroeugenol instead of from 4-propyl-2-methoxyclohexan-1-ol, which is the fully hydrogenated product. As a matter of fact, the energy barriers for the elementary steps of deoxygenation in the HYD mechanism are higher by about 40-50 kJ mol^{-1} than the corresponding ones in the DDO mechanism.

[Figure 6 about here.]

However, these inferences do not allow us to identify the path and, on the whole, the fastest mechanism. Therefore, all DFT information was used for an equilibrium microkinetic analysis that employs a new approach, called *Simplified Christiansen Method* (SCM), inspired by Christiansen's algebraic scheme [37], already applied for kinetic analyses of experimental catalytic results [38–41]. Indeed, by using as input the DFT values of the direct and inverse energy barriers characterizing the formation of surface species and the desorption energies of reactant and product, the SCM approach returns us the kinetic constants of the different pathways at the selected temperatures.

In order to consider the influence of temperature on reaction rates and desorption processes, the SCM was carried out in terms of Gibbs free energy. The comparison between the data reported in Tables 1 — where the Gibbs free energy variations of all the elementary steps occurring on both the HYD and DDO pathways have been collected — and Table 2, shows that the use of Gibbs free energies has a more significant effect on the desorption of stable species than on energy barriers.

11

[Table 1 about here.]

[Table 2 about here.]

The SCM results highlight, as detailed in Table 3, that the pathways in the DDO mechanism are at least two orders of magnitude faster than those in the HYD mechanism. In particular, the HYD-1 pathway, which involves the formation of propylcyclohexane through 4-propylcyclohexan-1-ol, is the fastest HYD pathway. On the other hand, the HYD-2 and HYD-3 pathways appear to be competitive with each other since, except for the temperature range 673-973 K, they always differ by an order of magnitude. The slowest of the HYD pathways is the fourth, HYD-4, most likely due to the high energy barriers for the formation of 4-propylcyclohexane-1,2-diol and the C$-$OH bond cleavage from it. This pathway, however, exhibits a faster rate compared to DDO-3, which is the slowest pathway within the DDO mechanism and, consequently, the slowest overall.

[Table 3 about here.]

At all investigated temperatures, and especially at high temperatures, the HDO reaction of isoeugenol on Pt_{10} appears to proceed essentially via the first DDO pathway, i.e., the one that runs through the 4-propylphenol intermediate in the first deoxygenation step. According to the SCM results, this pathway is about eight orders of magnitude faster than the fastest of the HYD mechanisms. Among the pathways involving the 1-methoxy-3-propylbenzene species, DDO-2, where the breaking of the C$-$OCH$_3$ bond occurs as an additional deoxygenation step, is significantly favored over DDO-3 which, as already anticipated, is the slowest pathway. The DDO-2 and DDO-4 pathways are somewhat competitive with each other, and the difference between their kinetic constants decreases as the temperature increases.

5. Conclusion

The growing demand for renewable and sustainable alternative energy sources has steered scientific research toward the study of one of the most promising routes for the valorization of biomass-derived bio-oils: hydrodeoxygenation, HDO. In the first paper of this series we investigated the properties of a Pt_{10} cluster, already experimentally focused as one of the best platinum cluster in hydrogenation reaction, to be used as catalyst model, In details, it has been considered: i) its interactions with of a isoeugenol, likely the most representative among biomass compounds, ii) its capability to fragment the hydrogen molecule and make atomic hydrogen available on its centers and finally iii) its ability to catalyze the transformation of isoeugenol to propylcyclohexane through the direct deoxygenation, DDO, pathway. In order to provide a comprehensive mapping at the atomistic level of the main mechanisms involved in the HDO process, in the present work the deoxygenation-through-hydrogenation pathway is reported, together with a conclusive systematic comparison between the two alternative mechanisms above.

Indeed, the detailed energetics of the two studied mechanisms, along with most of their possible routes, enabled us to conduct a Christiansen-like microkinetic analysis which, on the basis of the DFT-calculated forward/backward energy barriers and adsorption/desorption energetics, returns an unbiased guess of the kinetic constants at given temperatures. The kinetic data confirm the thermodynamic hypotheses that the DDO mechanism is the preferred one in the temperature range 473-973 K. In particular, subjected to molecular hydrogen flux the reaction should proceed through the formation of the 4-propylphenol intermediate, by the preferential removal of the methoxy fragment hence methanol, to give the final product, propylcyclohexane. In doing this, the the removal of the hydroxyl group, which desorbs as water, also occurs. Further, kinetic data suggest that the route implying the formation of methane could become competitive at higher temperature, while those channels involving 1-methoxy-3-propylbenzene as intermediate are ruled out, being the one passing through

3-propylphenol the slowest at all.

This work provides an almost complete mapping of the HDO mechanism of isoeugenol on a representative subnanometer platinum cluster and can be used as reference for further investigation. In particular, future works must be devoted on one side to evaluate the effect of supports and of the employment of different, namely less noble, metals on the key-point of the reaction, and on another side to ascertain if under molecular hydrogen flux the hydrodeoxygenation is actually preferred to the various decomposition modes that can be expected for molecules with many functional groups on metals hence would represent the most important processes in absence of hydrogen.

Acknowledgements

References

[1] Renewable energy: Power for a sustainable future (3rd ed.), published by Oxford University Press, Oxford in association with The Open University, Milton Keynes (September 2012).

[2] M. N. Uddin, K. Techato, J. Taweekun, M. M. Rahman, M. G. Rasul, T. M. I. Mahlia, S. M. Ashrafur, An overview of recent developments in biomass pyrolysis technologies, Energies 11 (2018). doi:https://doi.org/10.3390/en11113115.

[3] A. Gutierrez, R. Kaila, M. Honkela, R. Slioor, A. Krause, Hydrodeoxygenation of guaiacol on noble metal catalysts, Catal. Today 147 (2009) 239–246. doi:https://doi.org/10.1016/j.cattod.2008.10.037.

[4] J. Chang, T. Danuthai, S. Dewiyanti, C. Wang, A. Borgna, Hydrodeoxygenation of guaiacol over carbon-supported metal catalysts, ChemCatChem 5 (2013) 3041–3049. doi:https://doi.org/10.1002/cctc.201300096.

[5] C.-C. Chiu, A. Genest, A. Borgna, N. Rösch, Hydrodeoxygenation of guaiacol over Ru(0001): A DFT study, ACS Catalysis 4 (2014) 4178–4188. doi:10.1021/cs500911j.

[6] A. Bjelić, M. Grilc, B. Likozar, Catalytic hydrogenation and hydrodeoxygenation of lignin-derived model compound eugenol over Ru/C: Intrinsic microkinetics and transport phenomena, Chem. Eng. J. 333 (2018) 240–259. doi:https://doi.org/10.1016/j.cej.2017.09.135.

[7] M. Bertero, G. de la Puente, U. Sedran, Fuels from bio-oils: Bio-oil production from different residual sources, characterization and thermal conditioning, Fuel 95 (2012) 263–271. doi:https://doi.org/10.1016/j.fuel.2011.08.041.

[8] J. A. Maga, I. Katz, Simple phenol and phenolic compounds in food flavor, Crit. Rev. Food Sci. Nutr. 10 (1978) 323–372. doi:https://doi.org/10.1080/10408397809527255.

[9] D. Mohan, C. U. Pittman, P. H. Steele, Pyrolysis of wood-biomass for bio-oil: A critical review, Energy Fuels 20 (2006) 848–889. doi:https://doi.org/10.1021/ef0502397.

[10] G. W. Huber, S. Iborra, A. Corma, Synthesis of transportation fuels from biomass: Chemistry, catalysts, and engineering, Chem. Rev. 106 (2006) 4044–4098. doi:https://doi.org/10.1021/cr068360d.

[11] P. Mäki-Arvela, D. Y. Murzin, Hydrodeoxygenation of lignin-derived phenols: From fundamental studies towards industrial applications, Catalysts 7 (2017). doi:https://doi.org/10.3390/catal7090265.

[12] A. Bridgwater, Renewable fuels and chemicals by thermal processing of biomass, Chem. Eng. J. 91 (2003) 87–102. doi:https://doi.org/10.1016/S1385-8947(02)00142-0.

[13] K. Lee, G. H. Gu, C. A. Mullen, A. A. Boateng, D. G. Vlachos, Guaiacol hydrodeoxygenation mechanism on Pt(111): Insights from density functional theory and linear free energy relations, ChemSusChem 8 (2015) 315–322. doi:https://doi.org/10.1002/cssc.201402940.

[14] J. Lu, A. Heyden, Theoretical investigation of the reaction mechanism of the hydrodeoxygenation of guaiacol over a ru(0001) model surface, J. Catal. 321 (2015) 39–50. doi:https://doi.org/10.1016/j.jcat.2014.11.003.

[15] M. Hellinger, H. W. Carvalho, S. Baier, D. Wang, W. Kleist, J.-D. Grunwaldt, Catalytic hydrodeoxygenation of guaiacol over platinum supported on metal oxides and zeolites, Appl. Catal. A: Gen. 490 (2015) 181–192. doi:https://doi.org/10.1016/j.apcata.2014.10.043.

[16] C. González, P. Marín, F. V. Díez, S. Ordóñez, Gas-phase hydrodeoxygenation of benzaldehyde, benzyl alcohol, phenyl acetate, and anisole over precious metal catalysts, Ind. Eng. Chem. Res. 55 (2016) 2319–2327. doi:https://doi.org/10.1021/acs.iecr.6b00036.

[17] C. Nania, M. Bertini, L. Gueci, F. Ferrante, D. Duca, DFT insights into competing mechanisms of guaiacol hydrodeoxygenation on a platinum cluster, Phys. Chem. Chem. Phys. 25 (2023) 10460–10471. doi:10.1039/D2CP06077A.

[18] A. M. Barrios, C. A. Teles, P. M. de Souza, R. C. Rabelo-Neto, G. Jacobs, B. H. Davis, L. E. Borges, F. B. Noronha, Hydrodeoxygenation of phenol over niobia supported Pd catalyst, Catal. Today 302 (2018) 115–124. doi:https://doi.org/10.1016/j.cattod.2017.03.034.

[19] C. Zhao, J. He, A. A. Lemonidou, X. Li, J. A. Lercher, Aqueous-phase hydrodeoxygenation of bio-derived phenols to cycloalkanes, J. Catal. 280 (2011) 8–16. doi:https://doi.org/10.1016/j.jcat.2011.02.001.

[20] F. Ferrante, C. Nania, D. Duca, Computational investigation of isoeugenol transformations on a platinum cluster – I: Direct deoxygenation to propylcyclohexane, Mol. Catal. 529 (2022) 112541. doi:https://doi.org/10.1016/j.mcat.2022.112541.

[21] V. D'Anna, D. Duca, F. Ferrante, G. La Manna, DFT studies on catalytic properties of isolated and carbon nanotube supported Pd_9 cluster – I: adsorption, fragmentation and diffusion of hydrogen, Phys. Chem. Chem. Phys. 11 (2009) 4077–4083. doi:https://doi.org/10.1039/b820707k.

[22] V. D'Anna, D. Duca, F. Ferrante, G. La Manna, DFT studies on catalytic properties of isolated and carbon nanotube supported Pd_9 cluster: Part II. Hydro-isomerization of butene isomers, Phys. Chem. Chem. Phys. 12 (2010) 1323–1330. doi:https://doi.org/10.1039/b920949m.

[23] R. Schimmenti, R. Cortese, F. Ferrante, A. Prestianni, D. Duca, Growth of sub-nanometric palladium clusters on boron nitride nanotubes: a DFT study, Phys. Chem. Chem. Phys. 18 (2016) 1750–1757. doi:https://doi.org/10.1039/c5cp06625e.

[24] F. Ferrante, A. Prestianni, R. Cortese, R. Schimmenti, D. Duca, Density functional theory investigation on the nucleation of homo- and heteronuclear metal clusters on defective graphene, J. Phys. Chem. C 120 (2016) 12022–12031. doi:https://doi.org/10.1021/acs.jpcc.6b02833.

[25] T. Imaoka, Y. Akanuma, N. Haruta, S. Tsuchiya, K. Ishihara, T. Okayasu, W.-J. Chun, M. Takahashi, K. Yamamoto, Platinum clusters with precise numbers of atoms for preparative-scale catalysis, Nat. Comm. 8 (2017) 1–8. doi:https://doi.org/10.1038/s41467-017-00800-4.

[26] M. J. Frisch, G. W. Trucks, H. B. Schlegel, G. E. Scuseria, M. A. Robb, J. R. Cheeseman, G. Scalmani, V. Barone, G. A. Petersson, H. Nakatsuji, X. Li, M. Caricato, A. V. Marenich, J. Bloino, B. G. Janesko, R. Gomperts, B. Mennucci, H. P. Hratchian, J. V. Ortiz, A. F. Izmaylov, J. L. Sonnenberg, D. Williams-Young, F. Ding, F. Lipparini, F. Egidi, J. Goings, B. Peng, A. Petrone, T. Henderson, D. Ranasinghe, V. G. Zakrzewski, J. Gao, N. Rega, G. Zheng, W. Liang, M. Hada, M. Ehara, K. Toyota, R. Fukuda, J. Hasegawa, M. Ishida, T. Nakajima, Y. Honda, O. Kitao, H. Nakai, T. Vreven, K. Throssell, J. A. Montgomery, Jr., J. E. Peralta, F. Ogliaro, M. J. Bearpark, J. J. Heyd, E. N. Brothers, K. N. Kudin, V. N. Staroverov, T. A. Keith, R. Kobayashi, J. Normand, K. Raghavachari, A. P. Rendell, J. C. Burant, S. S. Iyengar, J. Tomasi, M. Cossi, J. M. Millam, M. Klene, C. Adamo, R. Cammi, J. W. Ochterski, R. L. Martin, K. Morokuma, O. Farkas, J. B. Foresman, D. J. Fox, Gaussian˜16 Revision C.01 (2016).

[27] A. D. Becke, A new mixing of Hartree–Fock and local density-functional theories, J. Chem. Phys. 98 (1993) 1372–1377. doi:https://doi.org/10.1063/1.464304.

[28] S. Grimme, J. Antony, S. Ehrlich, H. Krieg, A consistent and accurate ab initio parametrization of density functional dispersion correction

(DFT-D) for the 94 elements H-Pu, J. Chem. Phys. 132 (2010) 154104. doi:https://doi.org/10.1063/1.3382344.

[29] P. J. Hay, W. R. Wadt, Ab initio effective core potentials for molecular calculations. Potentials for the transition metal atoms Sc to Hg, J. Chem. Phys. 82 (1985) 270–283. doi:https://doi.org/10.1063/1.448799.

[30] P. J. Hay, W. R. Wadt, Ab initio effective core potentials for molecular calculations. Potential for K to Au including the outermost core orbitals, J. Chem. Phys. 82 (1985) 299–310. doi:https://doi.org/10.1063/1.448975.

[31] T. H. Dunning, P. J. Hay, Gaussian Basis Sets for Molecular Calculations, in: H. F. Schaefer (Ed.), Methods of Electronic Structure Theory, Modern Theoretical Chemistry, Springer US, 1977, pp. 1–27. doi:https://doi.org/10.1007/978-1-4757-0887-5-1.

[32] B. P. Pritchard, D. Altarawy, B. Didier, T. D. Gibson, T. L. Windus, New basis set exchange: An open, up-to-date resource for the molecular sciences community, J. Chem. Inf. Model. 59 (2019) 4814–4820. doi:https://doi.org/10.1021/acs.jcim.9b00725.

[33] S. F. Boys, F. Bernardi, The calculation of small molecular interactions by the differences of separate total energies. Some procedures with reduced errors, Mol. Phys. 19 (1970) 553–566. doi:https://doi.org/10.1080/00268977000101561.

[34] V. Fung, D.-E. Jang, Exploring structural diversity and fluxionality of Pt_n (n=10-13) clusters from first principles, J. Phys. Chem. C 121 (2017) 10796–10802. doi:https://doi.org/10.1021/acs.jpcc.6b11969.

[35] I. Demiroglu, K. Yao, H. A. Hussein, R. L. Johnston, DFT Global Optimization of Gas-Phase Subnanometer Ru–Pt Clusters, J. Phys. Chem. C 121 (2017) 10773–10780. doi:https://doi.org/10.1021/acs.jpcc.6b11329.

[36] L. Lozano, G. B. Marin, J. W. Thybaut, Analytical rate expressions accounting for the elementary steps in benzene hydro-

genation on Pt, Ind. Eng. Chem. Res. 56 (2017) 12953–12962. doi:https://doi.org/10.1021/acs.iecr.7b00742.

[37] J. Christiansen, The elucidation of reaction mechanisms by the method of intermediates in quasi-stationary concentrations, Vol. 5 of Adv. Catal., Academic Press, 1953, pp. 311–353. doi:https://doi.org/10.1016/S0360-0564(08)60644-6.

[38] L. Gueci, F. Ferrante, A. Prestianni, R. Di Chio, A. F. Patti, D. Duca, F. Arena, DFT insights into the oxygen-assisted selective oxidation of benzyl alcohol on manganese dioxide catalysts, Inorg. Chim. Acta 511 (2020) 119812. doi:https://doi.org/10.1016/j.ica.2020.119812.

[39] L. Gueci, F. Ferrante, A. Prestianni, F. Arena, D. Duca, Benzyl alcohol to benzaldehyde oxidation on MnO_x clusters: Unraveling atomistic features, Mol. Catal. 513 (2021) 111735. doi:https://doi.org/10.1016/j.mcat.2021.111735.

[40] L. Gueci, F. Ferrante, A. Prestianni, F. Arena, D. Duca, Structural, energetic and kinetic database of catalytic reactions: benzyl alcohol to benzaldehyde oxidation on MnO_x clusters, Data in Brief 38 (2021) 107369. doi:https://doi.org/10.1016/j.dib.2021.107369.

[41] F. Arena, F. Ferrante, R. Di Chio, G. Bonura, F. Frusteri, L. Frusteri, A. Prestianni, S. Morandi, G. Martra, D. Duca, DFT and kinetic evidences of the preferential CO oxidation pattern of manganese dioxide catalysts in hydrogen stream (PROX), Appl. Cat. B Env. 300 (2022) 120715. doi:https://doi.org/10.1016/j.apcatb.2021.120715.

TOC entry

Computational Investigation of Isoeugenol Transformations on a Platinum Cluster – II: Deoxygenation through Hydrogenation to Propylcyclohexane

Chiara Nania, Francesco Ferrante, Marco Bertini, Laura Gueci, Dario Duca
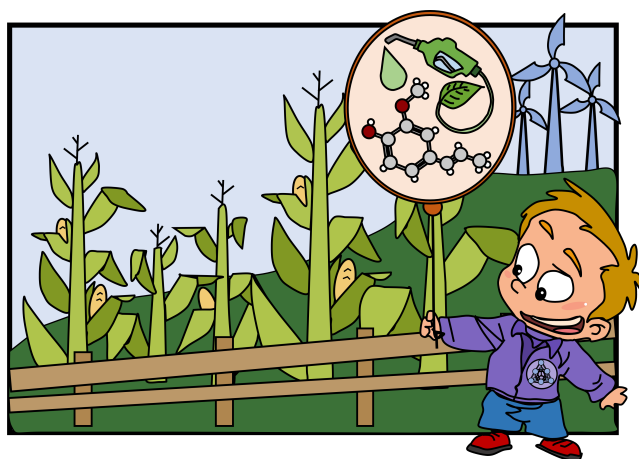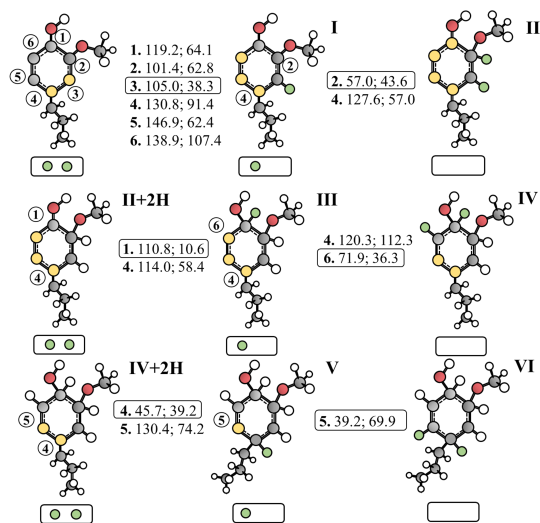
List of Figures

Figure 1: Schematic depiction of the full saturation of isoeugenol phenyl ring on the Pt_{10} cluster. The latter is represented by the small rectangle below the molecular species; adatoms are shown as green circles within the rectangle, those not-adsorbed are not shown; the yellow circles represent the interaction sites of the molecule with the cluster. In each entry, the first number represents the position where the catalytic hydrogen is added, the second is the energy barrier of the corresponding elementary step, and the third is the energy of the product, always taken with respect to the energy of the reactant with two H atoms still on Pt_{10}. All energy values are expressed in kJ mol^{-1}. The first hydrogenation starts from dihydroeugenol, the second from **II+2H** (6-methoxy-4-propylcyclohexa-1,3-dien-1-ol/$Pt_{10}2$H), the last from **IV+2H** (6-methoxy-4-propylcyclohex-3-en-1-ol/$Pt_{10}2$H) and leads to 2-methoxy-4-propylcyclohexan-1-ol/Pt_{10}.
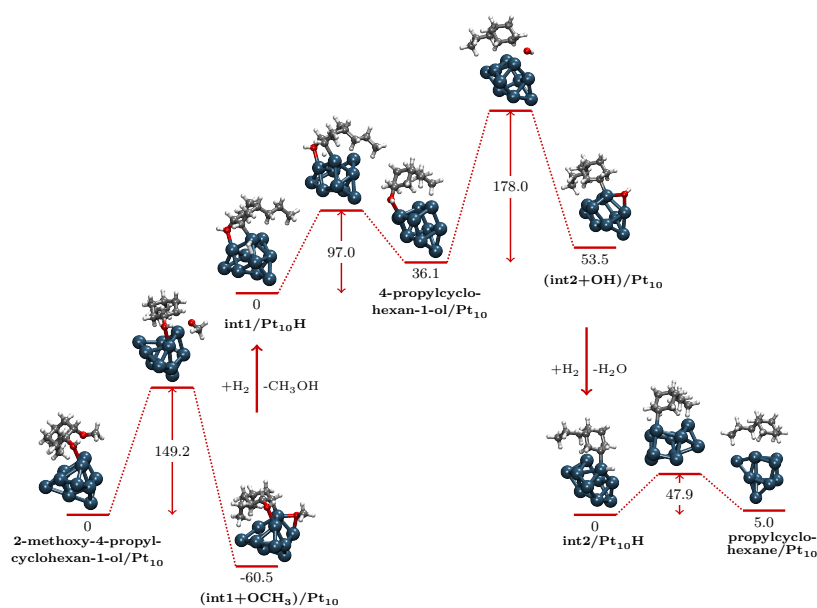
24

Figure 2: Reaction profile for HYD-1 mechanism, showing cleavage of the $C-OCH_3$ bond with adsorption of the OCH_3 fragment on a side edge of the cluster. After addition of one H_2 molecule and desorption of methanol, the formation of 4-propylcyclohexan-1-ol occurs, from which the $C-OH$ bond is broken. The OH fragment, by addition of another H_2 molecule, is hydrogenated and desorbed as H_2O. Finally, the hydrogenation of the unsaturated carbon, produces propylcyclohexane.
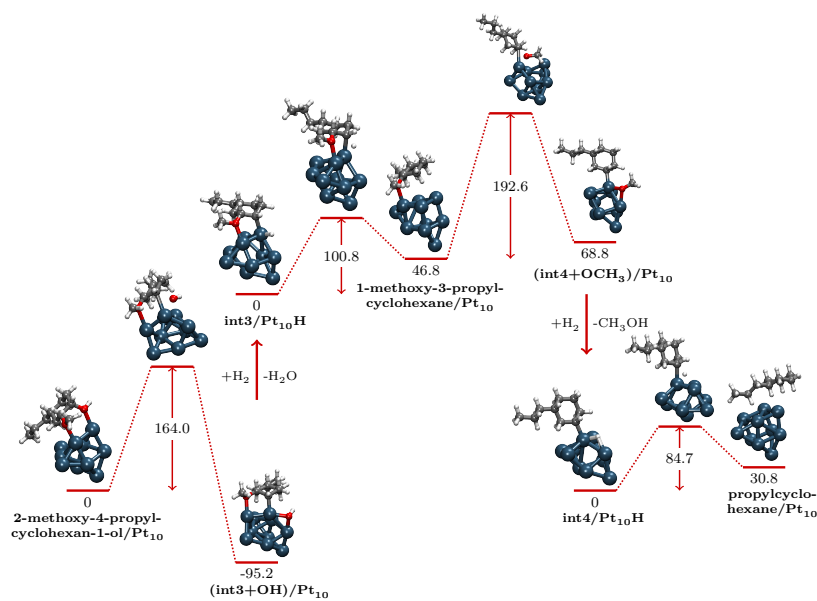
Figure 3: Reaction profile corresponding to the HYD-2 mechanism: breakage of the C−OH bond with adsorption of the OH fragment, hydrogenation of the unsaturated carbon with formation of 1-methoxy-3-propylcyclohexane, subsequent cleavage of the C−OCH$_3$ bond and hydrogenation of the unsaturated carbon atom to obtain propylcyclohexane. Fragmentation of two H$_2$ molecules is required for these stages.
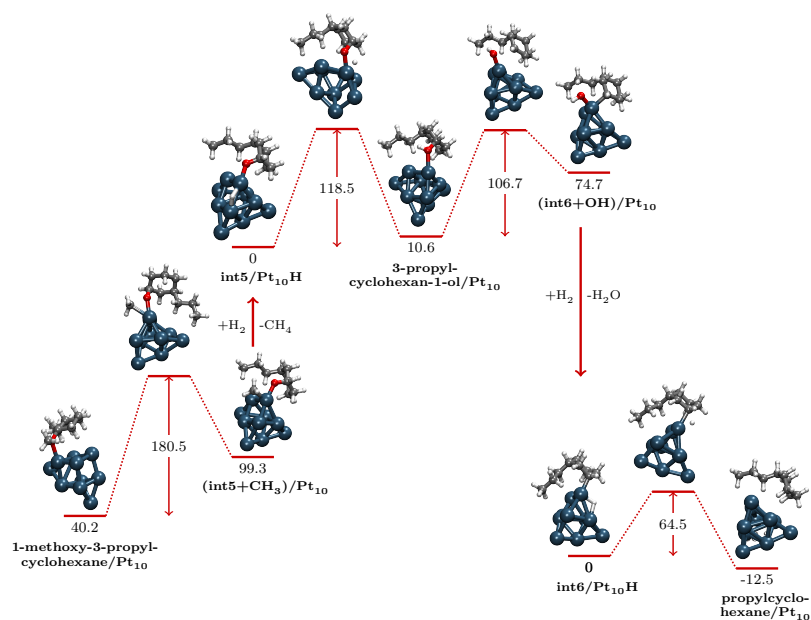
Figure 4: The reaction profile according with the HYD-3 mechanism, describes: cleavage of the $O-CH_3$ bond from the 1-methoxy-3-propylcyclohexane/Pt_{10}, hydrogenation of the CH_3 fragment with methane formation, and restoration of the $-OH$ functionality ruling the 3-propylcyclohexanol/Pt_{10} formation. From the latter, after the elimination of one water molecule, propylcyclohexane/Pt_{10} is formed by hydrogenation of the unsaturated carbon atom.
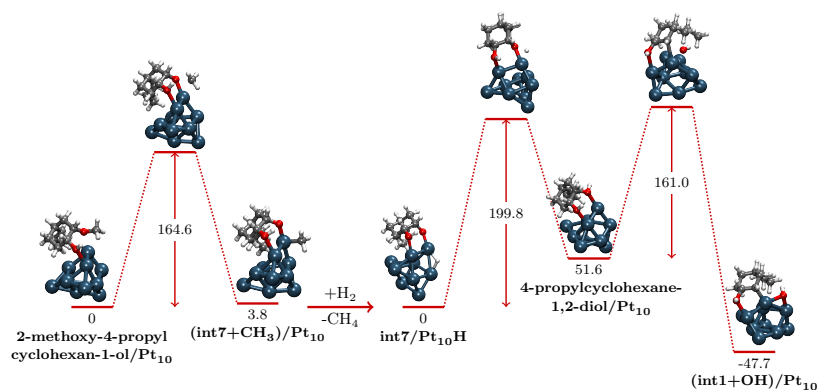
Figure 5: The reaction profile, which refers to the HYD-4 mechanism, involves the cleavage of the $O-CH_3$ bond in the methoxyl group with adsorption of the CH_3 fragment, which desorbs as methane after hydrogenation; a second H-atom is responsible for restoration of the $-OH$ functionality originating the 4-propylcyclohexane-1,2-diol/Pt_{10} species; this one evolves to 4-propylcyclohexane-1-ol/Pt_{10} as a result of the C-OH bond beaking. The 4-propylcyclohexane-1-ol/Pt_{10}, as detailed in Figure 2, leads to propylcyclohexane/Pt_{10}.
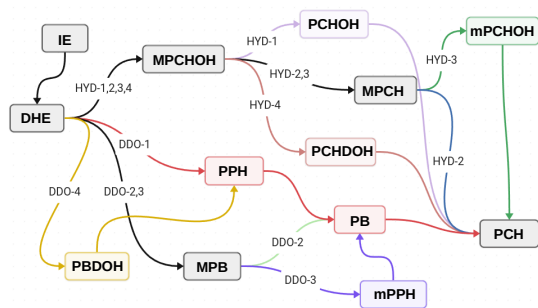
Figure 6: Visual overview of the eight most important pathways found for the isoeugenol hydrodeoxygenation reaction on Pt_{10}. The DDO mechanisms are those investigated in paper I. Legend: IE = isoeugenol; DHE = dihydroeugenol; MPCHOH = 2-methoxy-4-propylcyclohexan-1-ol; PCHOH = 4-propylcyclohexan-1-ol; MPCH = 1-methoxy-3-propylcyclohexane; PCHDOH = 4-propylcyclohexan-1,2-diol; mPCHOH = 3-propylcyclohexan-1-ol; PCH = 4-propylcyclohexane; PPH = 4-propylphenol; mPPH = 3-propylphenol; PB = 4-propylbenzene; MPB = 1-methoxy-3-propylbenzene; PBDOH = 4-propylbenzen-1,2-diol.

List of Tables

Table 1: Elementary reactions in the HYD and DDO mechanisms with the corresponding standard free energy barrier and reaction ΔG at T = 298.15 K.

Elementary process[a]	$\Delta G^{\#}$/kJ mol^{-1}	ΔG/kJ mol^{-1}
HYD pathways		
DHE/Pt$_{10}$2 H → I	105.7	41.2
I → II	60.6	-12.6
II+2H → III	109.4	9.9
III → IV	72.0	11.2
IV+2H → V	52.4	40.0
V → VI	35.6	-6.7
MPCHOH/Pt$_{10}$ → (int1+OCH$_3$)/Pt$_{10}$	148.3	-52.8
int1/Pt$_{10}$H → PCHOH/Pt$_{10}$	99.7	30.3
PCHOH/Pt$_{10}$ → (int2+OH)/Pt$_{10}$	180.3	17.3
int2/Pt$_{10}$H → PCH/Pt$_{10}$	49.3	7.9
MPCHOH/Pt$_{10}$ → (int3+OH)/Pt$_{10}$	167.5	-91.9
int3/Pt$_{10}$H → MPCH/Pt$_{10}$	99.0	40.2
MPCH/Pt$_{10}$ → (int4+OCH$_3$)/Pt$_{10}$	191.3	18.1
int4/Pt$_{10}$H → PCH/Pt$_{10}$	84.7	30.8
MPCH/Pt$_{10}$ → (int5+CH$_3$)/Pt$_{10}$	180.5	59.1
int5/Pt$_{10}$H → mPCHOH/Pt$_{10}$	114.6	4.6
mPCHOH/Pt$_{10}$ → (int6+OH)/Pt$_{10}$	168.3	65.3
int6/Pt$_{10}$H → PCH/Pt$_{10}$	65.0	-18.4
MPCHOH/Pt$_{10}$ → (int7+CH$_3$)/Pt$_{10}$	167.3	3.9
int7/Pt$_{10}$H → PCHDOH/Pt$_{10}$	187.1	43.3
PCHDOH/Pt$_{10}$ → (int1+OH)/Pt$_{10}$	167.3	-4.4
DDO pathways[b]		
IE/Pt$_{10}$2 H → int1/Pt$_{10}$H[a]	105.9	88.0
int1/Pt$_{10}$H[b] → DHE/Pt$_{10}$	119.3	48.6
DHE/Pt$_{10}$ → (int2+OCH$_3$)/Pt$_{10}$	116.9	-16.7
(int3+CH$_3$OH)/Pt$_{10}$2 H → (int4+CH$_3$OH)/Pt$_{10}$H	72.4	-56.6
int4/Pt$_{10}$H[b] → PPH/Pt$_{10}$	64.1	21.6
PPH/Pt$_{10}$ → (int5+OH)Pt$_{10}$	108.0	-5.7
int6/Pt$_{10}$H → PB/Pt$_{10}$	92.7	18.6
DHE/Pt$_{10}$ → (int2′+CH$_3$)/Pt$_{10}$	121.6	-32.4
int2′/Pt$_{10}$H[b] → PBDOH/Pt$_{10}$	101.8	68.7
PBDOH/Pt$_{10}$ → (int3′+OH)/Pt$_{10}$	114.4	-66.6
int3′/Pt$_{10}$H[b] → PPH/Pt$_{10}$	70.4	-14.3
DHE/Pt$_{10}$ → (int7+OH)/Pt$_{10}$	123.1[c]	27.1
int7/Pt$_{10}$H → MPB/Pt$_{10}$	69.5[c]	-15.3
MPB/Pt$_{10}$ → (int8+OCH$_3$)/Pt$_{10}$	118.9[c]	-20.4
int8/Pt$_{10}$H → PB/Pt$_{10}$	80.1[c]	-10.8
MPB/Pt$_{10}$ → (int9+CH$_3$)/Pt$_{10}$	198.1[c]	-41.2
int9/Pt$_{10}$H → mPPH/Pt$_{10}$	164.7[c]	105.8
mPPH/Pt$_{10}$ → (int10+OH)/Pt$_{10}$	156.2[c]	128.0
int10/Pt$_{10}$H → PB/Pt$_{10}$	156.2[c]	128
PB/Pt$_{10}$2 H → I	101.1	53.7
I → II	39.2	-11.6
II → III	84.3	36.0
III → V	82.4	31.3
V → IX	75.6	-54.9
IX → X[d]	110.7	27.6

[a] See Figure 6 for the shorthand notation employed for the chemical species.

[b] The detailed analysis of these pathways is reported in paper I.

[c] These elementary steps have not been published in paper I, but are reported here for the first time since they were included in the SCM analysis. They correspond to two alternative mechanisms leading to PB. Both are triggered by the C−OH bond breaking, with formation of methoxy-3-propylbenzene (MPB) and water after that one H$_2$ molecule fragments on the cluster. In the first bifurcation, MBP loses its −OCH$_3$ group and a second H$_2$ molecule gives rise to PB and methanol. In the second bifurcation, characterized by very high energy barriers, the O−CH$_3$ bond breaking occurs, leading to methane and 3-prophylphenol (mPPH), which then loses the −OH group as water on the way to PB, so requiring one H$_2$ molecule more than the first pathway.

[d] This corresponds to the PCH/Pt$_{10}$ species represented in Scheme 1 of paper I.

Table 2: Standard Gibbs free energies of desorption (T = 298.15 K) for the stable intermediates and products occurring in the investigated HYD pathway.

compound[a,d] / ΔG_{des}/kJ mol^{-1}			
IE[b]		130.2	
DHE[b]		85.3	
CP[b]		28.8	
HYD		**DDO**	
MPCHDEOH	190.7	PPH	91.1
MPCHEOH	131.9	PB	77.9
MPCHOH	40.4	MPB	105.9
MPCH	70.4	mPPH	80.1
mPCHOH	54.5	PBDOH	60.8
PCHOH	70.4	PCHDE	176.9
PCHDOH	55.8		
CH_3OH[c]	42.5	CH_3OH	23.6
H_2O	1.4	H_2O	50.4
CH_4	-11.8	CH_4	-70.9

[a] See Figure 6 for the shorthand notation employed for the chemical species; further, in this table the notation MPCHDEOH = 6-methoxy-4-propylcyclohexa-1,3-dien-1-ol; MPCHEOH = 6-methoxy-4-propylcyclohex-3-en-1-ol; PCHDE = 5-propyl-1,3-cyclohexadiene is used. Each molecule is intended adsorbed on the Pt_{10} cluster.

[b] These species are common to all pathways.

[c] ΔG_{des} of methanol, water and methane are different for HYD and DDO mechanisms because they desorb leaving different species adsorbed on the platinum cluster.

[d] The desorption process of the A species is $(A + X)/Pt_{10} \longrightarrow A + X/Pt_{10}$, being X a different species, if any, left adsorbed on the cluster.

Table 3: Reaction rates of the eight isoeugenol HDO mechanisms acording to SCM analysis at various temperature.
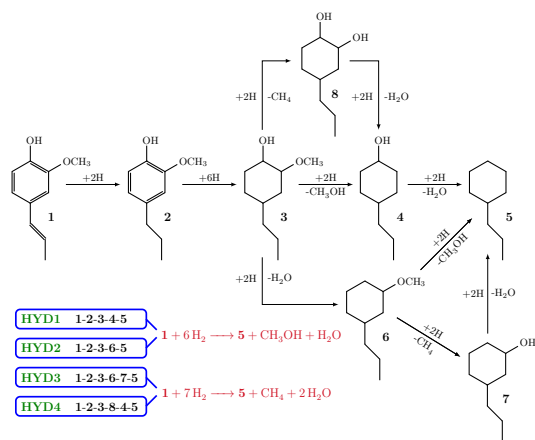
	Reaction rate[a]					
	473[b]	**573**	**673**	**773**	**873**	**973**
HYD-1	1.1(-24)	1.8(-18)	1.9(-14)	2.0(-11)	2.3(-9)	1.5(-7)
HYD-2	6.6(-26)	1.2(-19)	2.5(-15)	3.3(-12)	4.4(-10)	3.3(-8)
HYD-3	7.5(-27)	3.3(-20)	1.1(-15)	1.9(-12)	2.9(-10)	2.4(-8)
HYD-4	4.5(-31)	8.8(-24)	1.1(-18)	4.6(-15)	1.6(-12)	2.6(-10)
DDO-1	8.1(-16)	7.2(-11)	2.0(-7)	6.5(-5)	3.1(-3)	9.6(-2)
DDO-2	1.6(-22)	1.0(-16)	9.9(-13)	7.8(-10)	7.7(-8)	4.2(-6)
DDO-3	5.4(-46)	6.2(-36)	6.3(-29)	8.2(-24)	4.2(-20)	5.1(-17)
DDO-4	1.7(-20)	8.6(-15)	7.4(-11)	4.9(-8)	4.2(-6)	2.1(-4)

[a] Reaction rates are expressed in s^{-1}. The power of 10 of scientific notation is given in parenthesis. Gibbs free energies (as a function of temperature, at p = 1 atm) have been considered for the kinetic analysis.

[b] Temperatures in Kelvin.

List of Scheme

Scheme 1: Isoeugenol conversion to propylcyclohexane according to HYD mechanism: schematic representation of the four reaction pathways.